

IMPACT OF EARTH'S REFLECTED RADIATION ON ATTITUDE MOTION OF A NANOSATELLITE

Demet CILDEN-GULER,

*Department of Astronautics Engineering, Istanbul Technical University, Istanbul, Türkiye
cilden@itu.edu.tr*

Coarse sun sensors (CSSs) are widely used on nanosatellites for attitude estimation procedure. When the satellite is close enough to a planet, CSSs will be affected by the reflected radiation. The solar radiation not only provides illumination on the spacecraft but also exercises a torque on the craft. It is known that the spacecraft torques are small in magnitude. However, their accumulation in long time periods might be significant. The pressure exerted on the spacecraft depends on the incidence angle and the material of the surface in addition to the intensity of the light (solar power per unit area). In this study, only the fraction of the intensity is used from the albedo models by assuming that the incident radiation is always normal to the surface and the material is perfectly absorbing. That way the albedo model could be used for not only correcting the anomalous readings of CSSs but also modeling the reflected radiation pressure acting on the satellite roughly.

Key Words: sun sensor, reflected radiation, albedo, attitude, estimation

1. Introduction

The largest source of radiation in space is direct sunlight. Its value close to Earth can be used as approximately constant. It is observed that this value might change around 0.1% in low Earth orbits whereas 6 times larger in geostationary orbits¹. Especially for orbit propagation, shape or reflectivity properties are essential². In the study³, pose estimation is applied using artificial neural network. It is also stated that energy received by the surface of an Earth-orbiting satellite significantly depends on its position and orientation.

The cosine type photodiodes are commonly implemented as coarse sun sensors (CSSs) on cubesats, e.g. by placing one on each side in the study⁴. As different light sources cannot be isolated,

the albedo affects are suggested to be mitigated by employing three-axis magnetometer (TAM)⁴. However, it is also possible to correct the CSSs from the albedo effects without using TAM as stated in the research⁵. Different methods can be used for modeling CSS output by incorporating the Earth albedo model by Earth surface partitioning^{6,7}.

In this study, albedo model is not only used for correcting the CSS measurements but also used for modeling the torques caused by the reflected solar radiation, assuming that the material is perfectly absorbing.

2. Mathematical Models

CSSs based on the cosine type photodiodes outputs the

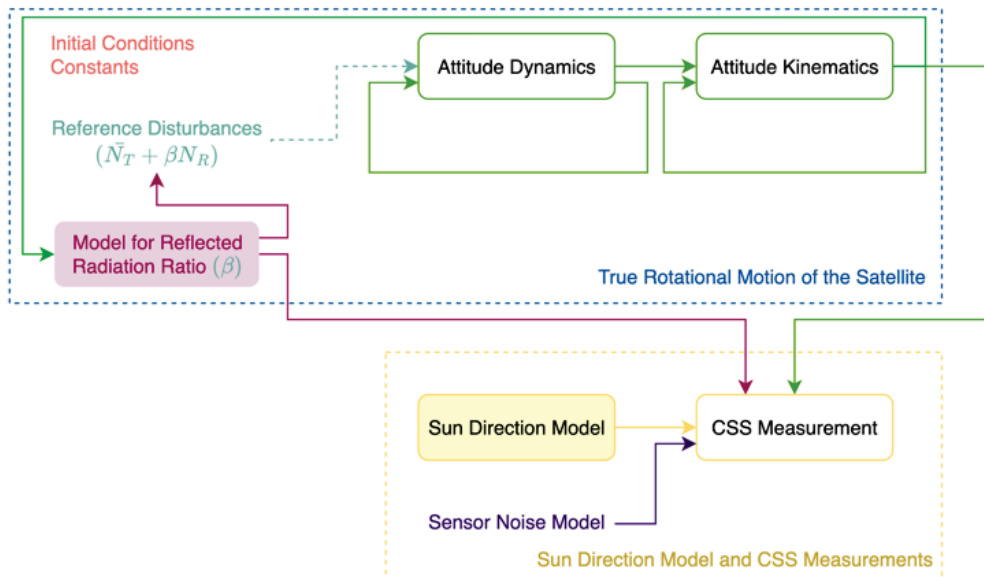


Fig. 1. True rotational motion and reference models for reflected radiation and sun direction.

currents proportional to the angle between the sensor's boresight and the direction of the light source⁸). The solar irradiance formulation on the sun sensor position is

$F_{\text{sun}}(\hat{\mathbf{s}}_{\text{SS}} \cdot \hat{\mathbf{n}}_{\text{SS}})$ where F_{sun} is the solar constant, $\hat{\mathbf{s}}_{\text{SS}}$ is the sun direction vector from the sun sensor, $\hat{\mathbf{n}}_{\text{SS}}$ is the unit normal vector of each sensor. The generated current of the sun sensor is then,

$$I_d = \begin{cases} I_{\text{max}} \frac{F_{\text{sun}}}{F_{\text{cal}}} (\hat{\mathbf{s}}_{\text{SS}} \cdot \hat{\mathbf{n}}_{\text{SS}}) & \text{if } (\hat{\mathbf{s}}_{\text{p}} \cdot \hat{\mathbf{n}}_{\text{A}} > 0) \cap (\hat{\mathbf{s}}_{\text{SS}} \cdot \hat{\mathbf{n}}_{\text{SS}} \geq \cos(\Delta)) \\ 0 & \text{otherwise} \end{cases} \quad (1)$$

where F_{cal} is the calibration flux determined in ground testing, I_{max} is the maximum output current of the sun sensor, $\hat{\mathbf{s}}_{\text{p}}$ is the sun direction vector from the celestial object, $\hat{\mathbf{n}}_{\text{A}}$ is the unit normal vector of the differential area on the celestial object, Δ is the half-field of view angle. The current of the sun sensor because of the albedo is⁷,

$$I_{\alpha} = \begin{cases} I_{\text{max}} \frac{F_{\text{sun}}}{F_{\text{cal}}} \sum_{i=1}^{N_A} \frac{\alpha (\hat{\mathbf{s}}_{\text{p}} \cdot \hat{\mathbf{n}}_{A_i}) (\hat{\mathbf{r}}_{\text{AS}_i} \cdot \hat{\mathbf{n}}_{A_i}) (-\hat{\mathbf{r}}_{\text{AS}_i} \cdot \hat{\mathbf{n}}_{\text{SS}})}{\pi \|\mathbf{r}_{\text{AS}_i}\|^2} \Delta A_i & \text{if } \Delta A \in A \\ 0 & \text{if } \Delta A \notin A \end{cases} \quad (2)$$

where \mathbf{r}_{AS} is the sun sensor's position vector from the differential area on the celestial body with the unit direction vector, α is the albedo coefficient of the celestial body.

By adding the albedo contribution on the sun sensor, the current of each sensor can be calculated as,

$$I = I_d + I_{\alpha} + \varepsilon_{\text{CSS}}, \quad (3)$$

where ε_{CSS} is zero-mean Gaussian noise on the measurements. For more than one CSS, the sun direction measurements can be summed up to the vector as,

$$\mathbf{y}_{\text{SS}} = \sum_{i=1}^{N_{\text{SS}}} I_i \cdot \hat{\mathbf{n}}_{\text{SS}_i}, \quad (4)$$

where N_{SS} is the number of CSSs.

The dynamic relations can be obtained by the principle of the conservation of angular momentum. By adding the acting external torques as,

$$J_1 \frac{d\omega_1}{dt} = N_1 + (J_2 - J_3) \omega_2 \omega_3, \quad (5)$$

$$J_3 \frac{d\omega_3}{dt} = N_3 + (J_1 - J_2) \omega_1 \omega_2 \quad (6)$$

$$J_2 \frac{d\omega_2}{dt} = N_2 + (J_3 - J_1) \omega_3 \omega_1, \quad (7)$$

where J_1 , J_2 and J_3 are the terms of the principal moment of inertia, N_1 , N_2 and N_3 are the terms of the external disturbances affecting the satellite. Solar radiation pressure (SRP) is one of the torques acting on the satellite, which also contains reflected radiation pressure as a summing term. The true rotational motion and reference models for the reflected radiation and the sun direction is presented in Fig. 1. An emphasis is given to the reflected radiation pressure modeling by using an albedo model.

3. Attitude Estimation Filter

The estimation problem in general state-space form is expressed as,

$$\mathbf{x}_k = f(\mathbf{x}_{k-1}) + \mathbf{w}_k, \quad (8)$$

$$\mathbf{y}_k = h_k(\mathbf{x}_k) + \varepsilon_k, \quad (9)$$

where $f(\cdot)$ is the process and $h(\cdot)$ is the measurement function, \mathbf{x}_k is the state vector at a time t_k , \mathbf{w}_k is the zero-mean Gaussian noise vector with the covariance of \mathbf{Q} , \mathbf{y}_k is the measurement vector, and ε_k is the zero-mean Gaussian noise vector with the covariance of \mathbf{R}_k .

The attitude of the satellite can be estimated using a Kalman-

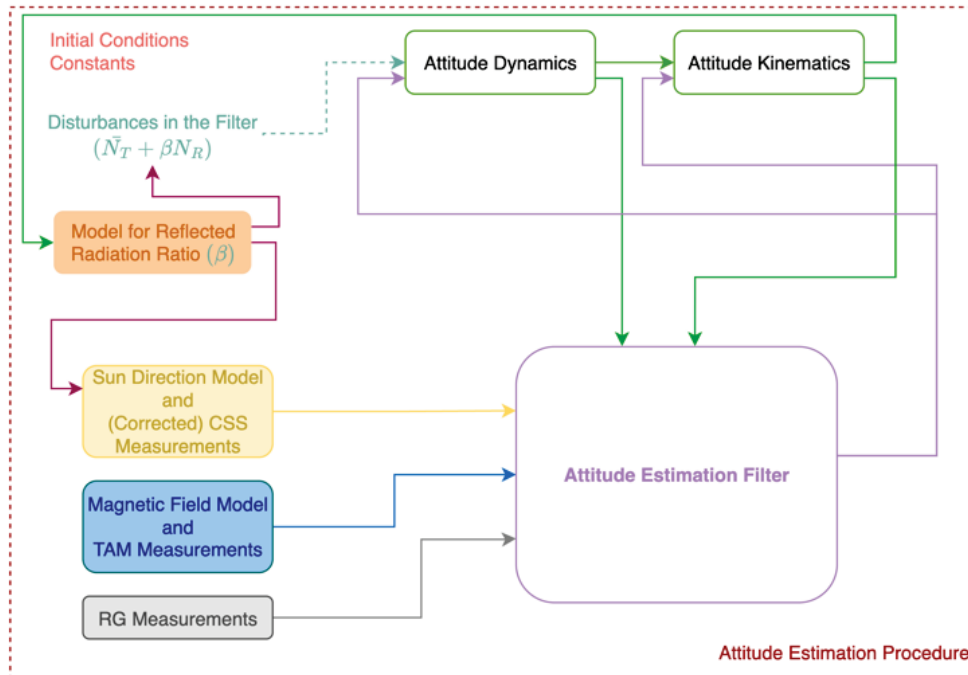


Fig. 2. Attitude estimation procedure based on CSS, TAM and RG measurements.

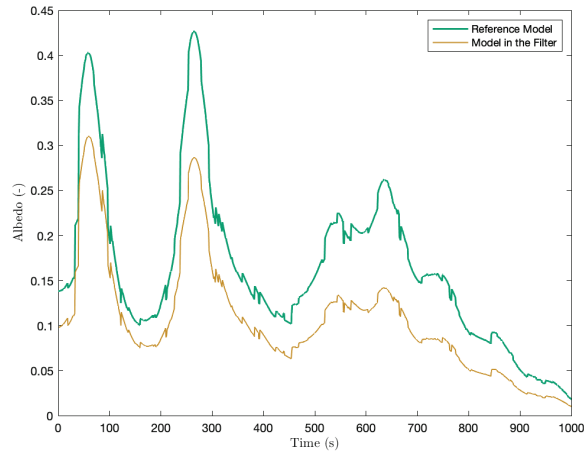


Fig. 3. Reflected radiation ratio reference models.

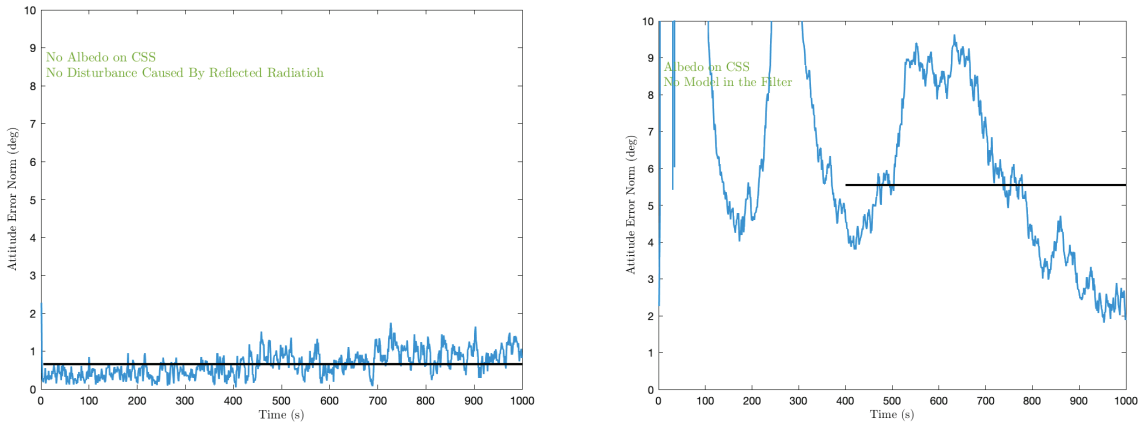


Fig. 4. (a) Albedo effects and disturbance caused by reflected radiation are disregarded (Case 0). (b) Albedo effects are considered but disturbances are disregarded (Case 1).

type filter using nonlinear process and measurement functions. In this study, we use sun and magnetic field directions with the CSSs and TAM measurements in the attitude estimation filter. The filter is based on a conventional extended Kalman filter (EKF), which also uses rate gyros in the filtering stage. The reflected radiation ratio is implemented by using the average albedo value (0.29) for the filter. The CSS measurements are modeled based on the sun direction model, albedo model and the noise model that are then processed under a Kalman-type filter with the rate gyro measurements for estimating the attitude.

4. Simulation Results

A nanosatellite is tumbling at near-polar low Earth elliptical orbit (630-850 km). The satellite has CSSs on each side, TAM and a rate gyro for attitude and rate measurements. EKF is used for attitude estimation filtering. The reflected radiation ratios are modeled using the complex albedo model based on the CERES data⁹⁾ for the reference model in true rotational motion simulation, and the simple albedo model based on the average value for the filtering as presented in Table 1. The figure containing reflected radiation ratios versus time is presented in

Fig. 3 for the reference model and the model in the filter. The trends of the models seem similar, yet the reference model has greater value all the time.

Table 1. Reflected radiation ratio models: Reference and filtering purposes.

| Model | Reflected Radiation Rate Data | Type of Average | Sky | Additional Comments |
|-----------|-------------------------------|-----------------|-------|---|
| Reference | CERES | 11-year average | Clear | |
| Filter | - | - | - | 0.29 for every differential area of Earth |

Six different cases are evaluated in the analysis. As the best-case scenario, we assumed there is no albedo on CSSs, and no disturbances caused by reflected radiation acting on the satellite. This case is called Case 0 and presented in Fig. 4(a). Then, the worst-case scenario is introduced by having the albedo effects without correcting the CSSs, which is presented in Fig. 4(b). As can be seen from the figure, the mean error is over 5 degrees in this case.

The CSSs are corrected by removing the albedo using the

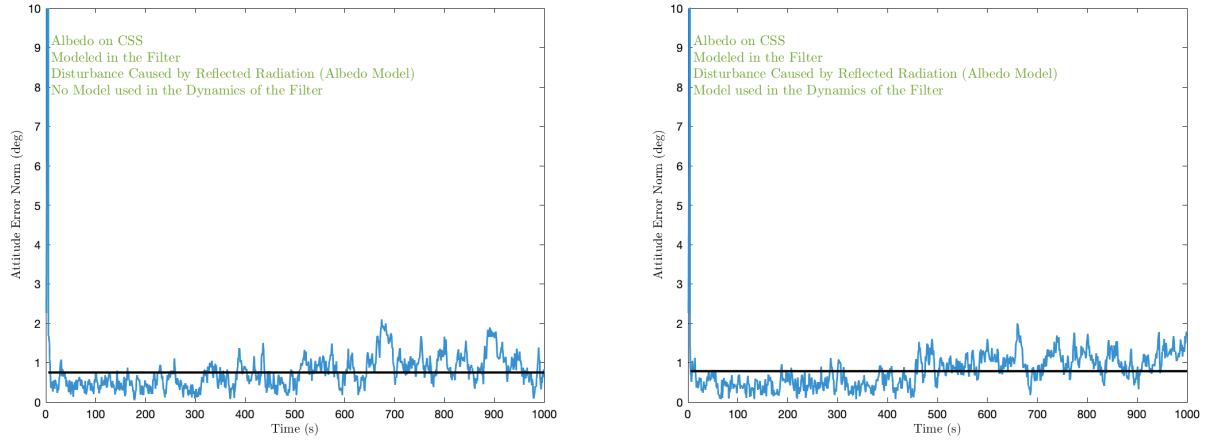


Fig. 5. CSS is corrected from albedo effects and disturbance is modeled based on albedo model. An albedo model is not used in the filter (Case 2a), a model is used in the filter (Case 2b).

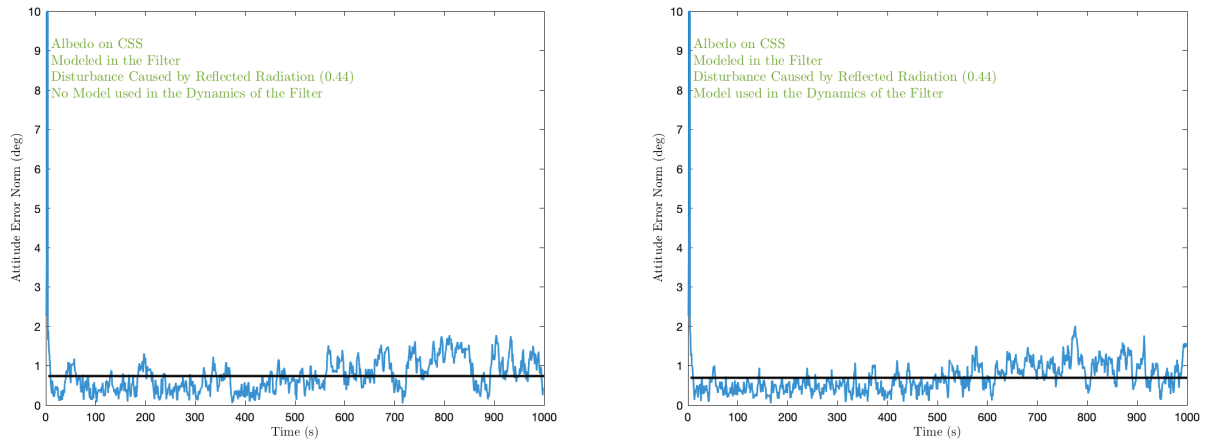


Fig. 6. CSS is corrected from albedo effects and disturbance is modeled based on average of 0.44. An albedo model is not used in the filter (Case 3a), a model is used in the filter (Case 3b).

model in the filter. First, any reflected radiation disturbance is not used in the filter for the Case 2a presented in the left panel of Fig. 5. The same albedo model used for CSSs in the filter is realized for reflected radiation pressure modeling as a coarse approximation in Case 2b presented in the right panel of Fig. 5.

Table 2. Attitude estimation errors for various cases (averaged over 50 simulations).

| Attitude (deg) | | |
|----------------|------------|-----------|
| | Mean Error | RMS Error |
| Case 0 | 0.659 | 0.608 |
| Case 1 | 5.546 | 4.401 |
| Case 2a | 0.785 | 0.733 |
| Case 2b | 0.751 | 0.697 |
| Case 3a | 0.737 | 0.687 |
| Case 3b | 0.692 | 0.640 |

In Case 3, the albedo model is altered to the 0.44 average for modeling the reflected radiation pressure in the true rotational motion model. Like in the previous scenario, first, reflected radiation disturbance is not considered in the filter (Case 3a) as presented in the left panel of Fig. 6. The same albedo model used for CSSs in the filter is realized for reflected radiation

pressure modeling as a coarse approximation in Case 3b presented in the right panel of Fig. 6.

Table 2 shows an overall analysis of each case averaged over 50 simulations. The table is composed of the mean and root mean square (RMS) errors of attitude estimation for the Cases 0, 1, 2a, 2b, 3a, and 3b. When the disturbance model caused by reflected radiation is modeled in the filter, the estimation results are improved as can be seen from the table for the cases from 'a' to 'b' (Case 2 and 3). However, adding a model to the filter or not having any reflected radiation disturbance do not affect the accuracy much (maximum 0.126 degrees in the mean). For future studies, more realistic true models for reflected radiation disturbance torque modeling can be realized.

5. Conclusion

The reflected radiation causes anomalous readings on the coarse sun sensors, also creates reflected radiation torque on the spacecraft close enough to a planet. In this paper, the albedo models are examined so that if they can be used for modeling the SRP caused by reflected radiation. The models are used to correct the CSSs in the attitude estimation procedure and model the disturbance torques. The attitude is estimated under 1-degree mean accuracy by the presented Kalman-type filter using TAMs and CSSs.

References

1. Hughes, P.C.: *Spacecraft Attitude Dynamics*. Mineola, New York: Dover Publications, 2004.
2. Friedman, A.M., Frueh, C.: Observability of Light Curve Inversion for Shape and Feature Determination Exemplified by a Case Analysis, *Journal of the Astronautical Sciences*, Vol. 69, Issue 2, 2022, pp. 537–569.
3. Nasihati Gourabi, F., Kiani, M., and Pourtakdoust, S.H.: Satellite pose estimation using Earth radiation modeled by artificial neural networks, *Advances in Space Research*, Vol. 70, Issue 8, 2022, pp. 2195–2207.
4. Frezza, L., Santoni, F., and Piergentili, F.: Sun direction determination improvement by albedo input estimation combining photodiodes and magnetometer, *Acta Astronautica*, Vol. 190, 2022, pp. 134–148.
5. Cilden-Guler, D., Schaub, H., Hajiyev, C., and Kaymaz, Z.: Attitude Estimation with Albedo Interference on Sun Sensor Measurements, *Journal of Spacecraft and Rockets*, Vol. 58, Issue 1, 2021, pp. 148–163.
6. O’Keefe, S.A. and Schaub, H.: Sun-direction estimation using a partially underdetermined set of coarse sun sensors, *Journal of the Astronautical Sciences*, Vol. 61, Issue 1, 2014, pp. 85–106.
7. Bhandari, D.: Modeling Earth Albedo Currents On Sun Sensors for Improved Vector Observation, *AIAA Guidance, Navigation, and Control Conference and Exhibit*, 2006. doi: 10.2514/6.2006-6592.
8. Flatley, T.W., and Moore, W.A.: An Earth Albedo Model: A Mathematical Model for the Radiant Energy Input to an Orbiting Spacecraft Due to the Diffuse Reflectance of Solar Radiation From the Earth Below, Technical Memorandum 104596, National Aeronautics and Space Administration, Goddard Space Flight Center, Greenbelt, MD, 1994.
9. Kato, S., Loeb, N.G., Rutan, D.A., and Rose, F.G.: Clouds and the Earth’s Radiant Energy System (CERES) Data Products for Climate Research, *Journal of the Meteorological Society of Japan*, Vol. 93, Issue 6, 2015, pp. 597–612.